Journal of Power Sources 460 (2020) 228107

Contents lists available at ScienceDirect

Journal of Power Sources

journal homepage: www.elsevier.com/locate/jpowsour

Conductivity, permeability, and stability properties of chemically tailored poly(phenylene oxide) membranes for Li^+ conductive non-aqueous redox flow battery separators

Patrick M. McCormack, Hongxi Luo, Geoffrey M. Geise **, Gary M. Koenig Jr. *

Department of Chemical Engineering, University of Virginia, 102 Engineers' Way, Charlottesville, VA, 22904, USA

HIGHLIGHTS

- Selective ion conducting membrane developed for non-aqueous electrochemical systems.
- Membranes stable for over four months in organic battery electrolyte.
- High conductivity in organic electrolyte relative to reported and control materials.
- Low redox shuttle crossover resulted in high membrane selectivity.
- Potential platform for non-aqueous redox flow battery separators.

GRAPHICAL ABSTRACT

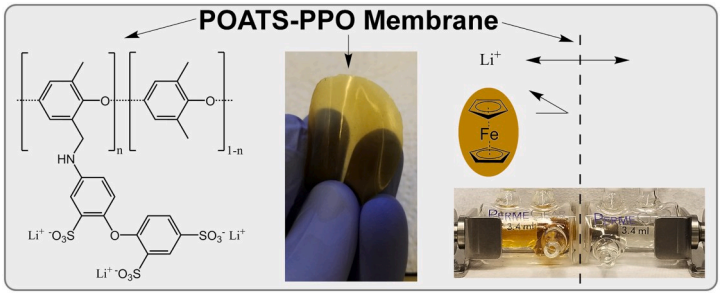

ARTICLE INFO

Keywords:
Non-aqueous flow battery
Lithium conducting membrane
Separator
Functional polymer
Energy storage

ABSTRACT

Non-aqueous redox flow batteries can operate at a higher voltage and energy density than aqueous systems, but developing these batteries will require new membrane separators engineered specifically for non-aqueous applications. Herein, we report the preparation and characterization of a series of membranes engineered specifically for a non-aqueous redox flow battery by functionalizing a poly(phenylene oxide) (PPO) backbone with increasing amounts of a highly sulfonated side chain, phenoxyaniline trisulfonate (POATS). These POATS-PPO membranes appear to be dimensionally stable over a period of at least four months in the non-aqueous electrolyte, and they exhibit lithium ion conductivities greater than that of previously reported control membranes. Ionic conductivity values, measured in non-aqueous and aqueous electrolytes, reveal solvent-specific ionic conductivity properties that differ from expected scaling relationships based on the ionic conductivity of the bulk electrolyte solution. The permeability of the membranes to ferrocene, a representative redox active molecule, does not change significantly with the degree of functionalization of the membrane. As a result, selectivity increases due to the increase in ionic conductivity as the degree of functionalization increases. Overall, the characterization of flow battery-relevant electrochemical properties suggests that these POATS-PPO membranes are promising materials for non-aqueous flow battery applications.

* Corresponding author. Department of Chemical Engineering, University of Virginia, 102 Engineers' Way P.O. Box 400741, Charlottesville, VA, 22904, USA.
** Corresponding author. Department of Chemical Engineering, University of Virginia, 102 Engineers' Way P.O. Box 400741, Charlottesville, VA, 22904, USA.
E-mail addresses: geise@virginia.edu (G.M. Geise), gary.koenig@virginia.edu (G.M. Koenig).

https://doi.org/10.1016/j.jpowsour.2020.228107
Received 7 December 2019; Received in revised form 13 March 2020; Accepted 24 March 2020
Available online 8 April 2020
0378-7753/

1. Introduction

Rising usage of renewable energy sources has created a challenge for the electrical grid because the power provided by many renewable sources can be intermittent and out of the control of power plant operators [1]. Grid scale energy storage technologies are needed to resolve differences in energy supply and demand both on short time scales and through daily supply and demand cycles. Redox flow batteries (RFBs) (Fig. 1) are one potential grid scale energy storage solution [1–6]. In this design, battery energy and power are determined by the electrolyte volume and by the electrode and membrane area, respectively, and thus energy and power are often considered decoupled. This enables modular and scalable designs for applications with large capacity and long duration of delivered power.

Aqueous RFBs are available commercially, but using water as the solvent is not without drawbacks. The electrochemical stability window of water is relatively small (i.e., generally taken to be the thermodynamic value of 1.23 V, although certain salts and electrode materials can slightly increase this value), and operating a battery at low voltage limits the battery energy density [3,6]. Using a non-aqueous (organic) solvent instead of water expands the electrochemical stability window and enables a larger maximum voltage per cell. In addition, a diverse range of organic redox active molecules are highly soluble in organic solvents [4,5]. These organic electroactive materials can offer tunable redox potentials through substituent modification. Additionally, they are often more soluble than their aqueous analogs, and the ability to concentrate active material in the solvent increases energy density [7–10].

Studies have investigated potential redox couples for non-aqueous RFBs [4,11,12], but less attention has been given to the membrane separator that is required in these batteries. For the battery to operate, a charge carrier needs to selectively transport from one half of the battery to the other to balance the movement of electrons in the battery. Importantly, the membrane must transport these charge carriers while simultaneously preventing the transport (or crossover) of the redox active molecule. This crossover can cause self-discharge and a permanent loss of battery capacity [3].

Most studies on non-aqueous RFB test cells have used either nanoporous, microporous, or ion-exchange membrane (IEM) separators. Nanoporous and microporous separators provide favorable ionic conductivity but may do little to prevent crossover, particularly for some active species [11,13,14]. IEMs can provide better crossover resistance but often provide lower conductivity than their nanoporous counterparts, resulting in a high internal resistance and low energy efficiency. Some currently used IEMs include Nafion®, a perfluorinated cation exchange membrane [15,16], and a Neosepta AHA anion exchange membrane [13,17], but both of these membranes were designed for use in aqueous systems, which may lead to sub-optimal performance in non-aqueous systems. Other options include porous separators, which can exhibit high crossover unless solid suspensions of active materials are used [7,18,19], or ceramic membranes, which are brittle and can sometimes react with the redox active molecule [20]. Improving the performance of non-aqueous flow batteries will require a purpose-designed membrane that achieves both high conductivity and low crossover in non-aqueous electrolytes. This could be achieved through lowering the crossover in nanoporous membranes, or by increasing the conductivity of an IEM, which is the focus of this investigation.

A sensible starting point for designing a membrane for non-aqueous applications is to consider membranes designed for aqueous systems, given the large body of literature available, but this approach comes with challenges. Non-aqueous solvents can interact more favorably with polymers compared to water, causing some membranes to swell excessively in non-aqueous electrolytes [15,17]. Also, little is known about how the difference in solvent interactions affect ion transport properties in the new electrolyte. Our approach was to start with a rigid, high-glass transition temperature polymer (to resist swelling) and then to functionalize it with fixed negatively charged groups to promote cation conduction. The ionic conductivity properties were measured in both an organic and aqueous electrolyte to observe how solvent-specific interactions affected the ion transport properties of the membrane.

In this study, poly(phenylene oxide) (PPO) was functionalized with a highly sulfonated side chain to create a cation exchange membrane for non-aqueous RFB applications. PPO was chosen as the base polymer for its chemical stability, relatively established modification procedure, and high glass transition temperature [21–24]. Previously, PPO has been reported as the base polymer for cation and anion exchange membranes

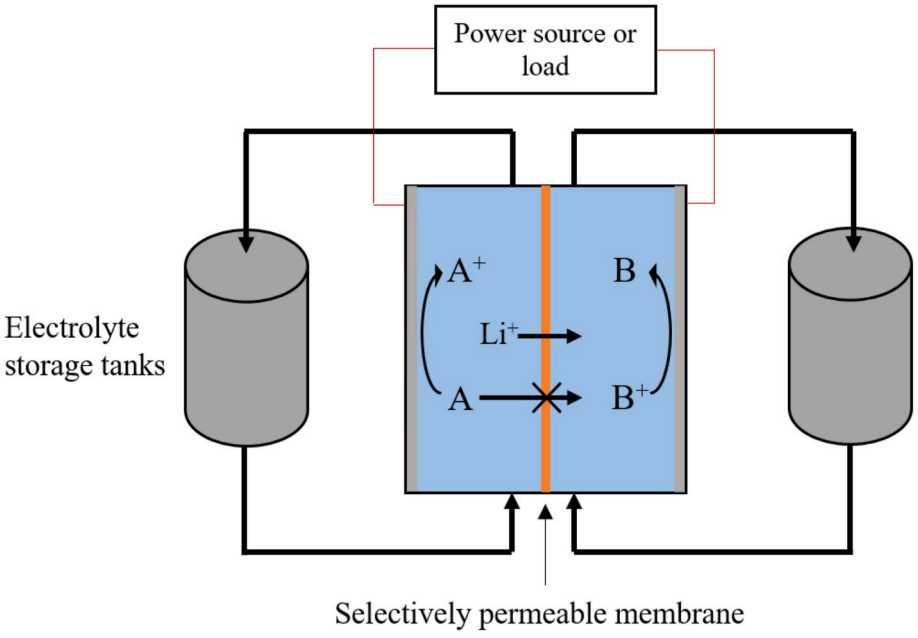

Fig. 1. Redox flow battery schematic. Electrochemical energy facilitated through redox active molecules ("A" and "B") dissolved in the electrolyte, and Li^+ shown as the charge carrier. During charge/discharge, electrolyte is pumped from the storage tanks through a flow cell containing electrodes and a selectively permeable membrane. An ideal membrane allows fast transport of the charge carrier while inhibiting transport of the redox active molecules.

in aqueous applications and for an anion exchange membrane in a non-aqueous application [21,25,26]. Here, a phenoxyaniline tri-sulfonate (POATS) side chain was attached to the polymer to introduce negatively charged fixed groups to promote cation conduction. POATS was chosen due to its chemical similarity to PPO and high charge density, which could increase charge carrier concentration and may induce some level of nano- or micro-phase separation, which could improve conductivity [27]. Since POATS-PPO membranes are cation exchange membranes, results were compared to a Nafion® 117 membrane and a Nafion®/polyvinylidene difluoride (PVDF) blended membrane previously evaluated within the context of non-aqueous flow batteries [20]. The desired charge carrier in the membrane was Li^+, and thus, all membranes were lithiated (i.e., converted to the lithium counter-ion form) before any measurements were made.

A wide range of non-aqueous flow battery electrolytes have been reported, and in this study, 1 M lithium bis(fluorosulfonyl)imide (LiFSI) in dimethyl carbonate (DMC) was used. LiFSI has been shown to be stable and have a high ionic conductivity in carbonate-based electrolytes, making it suitable for high rate applications, which is generally desirable for RFBs [28,29]. DMC was chosen because LiFSI is highly soluble in this solvent (up to 5 M), and of the carbonate solvents, dimethyl carbonate has a particularly low viscosity (0.59 cP), which could help to limit pumping losses in a flow battery [30,31]. All membranes were also tested in an aqueous electrolyte, 1 M LiCl, to determine how membrane properties are affected by the different solvent environments.

2. Methods

2.1. Phenoxyaniline trisulfonate (POATS) synthesis

POATS was synthesized by the aromatic sulfonation of phenoxyaniline. The procedure was adapted from a previous report [32] and is shown schematically in Scheme 1. In an ice bath, 15 mL fuming sulfuric acid (20% free SO_3 basis, Sigma Aldrich) was added slowly to a flask containing 2.0 g of 4-phenoxyaniline (97%, Sigma Aldrich). After the phenoxyaniline dissolved, the temperature was raised gradually to 80 °C over 30 min. After 2 h at 80 °C, the solution was poured over 80 g of ice prepared from deionized (DI, 18.2 Ω cm, Direct-Q 3 UV, Millipore) water and then diluted to a total volume of 500 mL using DI water. The triethylammonium cation was added to the solution as 4.5 mL triethylamine (>99%, TCI chemicals), and then calcium carbonate (>99%, Sigma Aldrich) was added until the solution became neutral. The precipitated calcium sulfate was removed by filtration, and the solution was dried in a rotary evaporator to obtain a crystalized product. The solids were re-dissolved in 10 mL DI water, boiled, and filtered to remove additional calcium sulfate and calcium carbonate precipitates. The POATS product was dried in a convection oven at 80 °C and stored in a dry box until use.

2.2. Brominated-poly(phenylene oxide) synthesis

Poly(2,6-dimethyl-1,4-phenylene oxide), PPO, was brominated using a free radical reaction to produce Br-PPO (Scheme 2) [22]. The bromine source was *N*-bromo-succinimide (NBS, 99%, Sigma Aldrich), and the initiator was azobisisobutyronitrile (AIBN, 98%, Sigma Aldrich). A typical reaction recipe was 6.0 g PPO (50 meq PPO repeat units, powder (SKU 181781), Sigma Aldrich), 2.23 g NBS (12.5 mmol), and 0.125 g AIBN (0.75 mmol). All reactants were dissolved in 75 mL chlorobenzene (Fisher Scientific) at room temperature, placed in an oil

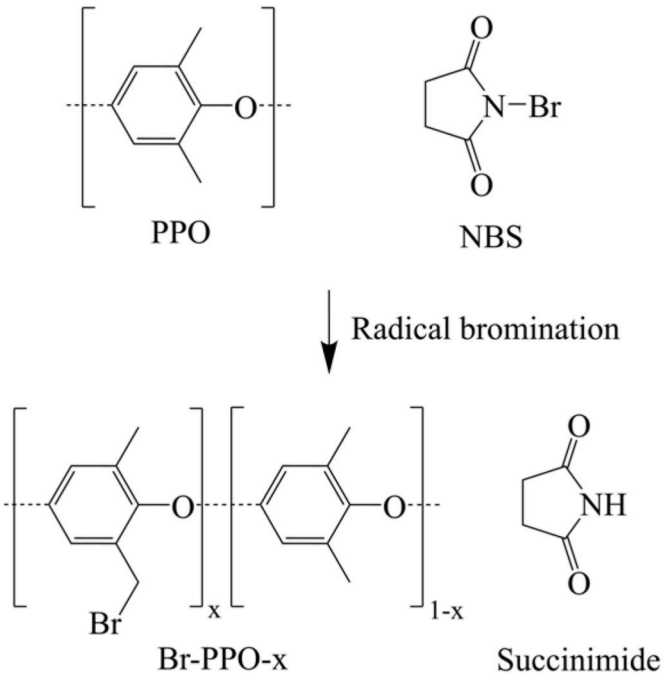

Scheme 2. Bromination of PPO to form Br-PPO

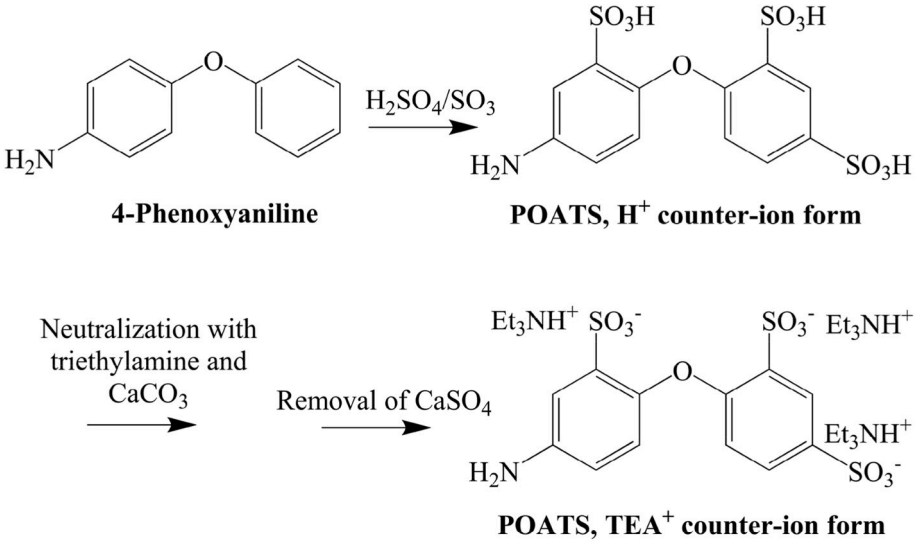

Scheme 1. POATS synthesis.

bath, and heated at 110 °C for 1 h. The solution subsequently was cooled to room temperature in a water bath, and the Br-PPO was precipitated in 10-fold excess reagent alcohol (Fisher Scientific) and collected via filtration. Then, the polymer was dried, re-dissolved in 50 mL chloroform (ACS reagent, Macron), and collected again by precipitation in reagent alcohol and filtration. Finally, the Br-PPO was dried under vacuum and stored until use. Although 25% bromination was theoretically possible with these example amounts, the reaction yielded an approximately 9% brominated product. The NBS and AIBN amounts were scaled to obtain different degrees of bromination.

2.3. Membrane synthesis

Br-PPO was reacted with POATS to convert Br-PPO to POATS-PPO (Scheme 3). To protect the reaction from water contamination, all materials and glassware initially were dried under vacuum. First, 0.3 g Br-PPO and 25% excess POATS were dissolved separately in 6 mL chlorobenzene and 12 mL anhydrous N-methyl-2-pyrrolidone (NMP, anhydrous, 99.5%, Sigma Aldrich), respectively. The solutions were added together into a two-necked flask along with 10 mg NaI (>99%, Sigma Aldrich) and 100% excess K_2CO_3 (>99%, Sigma Aldrich). The flask was placed in a 70 °C oil bath, and the reaction was allowed to proceed for 1 h under a dry nitrogen blanket. The polymer was precipitated in 150 mL of reagent alcohol, collected using a centrifuge, washed with a further 150 mL of reagent alcohol, collected again with a centrifuge, and dried under vacuum. Membranes were cast by dissolving 0.15 g of POATS-PPO in a mixture of 6 mL NMP and 3 mL chlorobenzene, casting this solution in a 6.5 cm diameter circular PTFE mold, and then drying the membranes for 16 h in a convection oven at 70 °C followed by 24 h under vacuum at 80 °C. Membranes were lithiated (i.e., exchanged into the lithium counter-ion form) by soaking each membrane in 100 mL of aqueous 1 M LiCl (>99%, Sigma Aldrich) solution for 24 h at 80 °C. The LiCl solution was replaced with fresh solution after the first 4 h of the soaking process.

2.4. Nafion® 117 pretreatment

The Nafion® 117 membrane was pretreated and converted to the lithium counter-ion form using a previously reported procedure [16]. First, the membrane was soaked in 3 wt% H_2O_2 (ACS reagent, Sigma Aldrich) for 1 h at 80 °C. The membrane then was soaked in aqueous 0.25 M H_2SO_4 (ACS reagent, Sigma Aldrich) at 80 °C for 1 h. Next, the membrane was lithiated by soaking the membrane in aqueous 0.25 M LiOH (Laboratory grade, Fisher Scientific) at 80 °C for 1 h. Finally, the membrane was soaked in 80 °C DI water 3 times for 30 min each time. The membrane was dried first in a convection oven at 80 °C for 6 h and then under vacuum at 80 °C overnight for approximately 16 h.

2.5. Nafion®/PVDF membrane synthesis

The Nafion®/PVDF membrane was prepared according to a previously reported procedure [20]. Nafion® 117 and Nafion® 212 have the same IEC and differ only in casting methods and thickness [33,34], so Nafion® 212 was used to increase surface area and accelerate dissolution. First, the Nafion® 212 membrane and PVDF powder were dried under vacuum for 24 h. After drying, 350 mg of Nafion® 212 was cut into small pieces, heated, and dissolved in 10 mL N, *N*′-dimethylformamide (>99%, Sigma Aldrich) at 80 °C in an oil bath. This process typically required 6 h. Then, an equal mass (350 mg) of PVDF (Kureha Corporation) was dissolved in the solution, and the mixture was left stirring in an 80 °C oil bath for 16 h to fully mix. The membrane was cast in a 10 cm diameter circular PTFE mold and dried at 80 °C for 12 h followed by 120 °C for 24 h. The membrane was hydrated with DI water and peeled from the mold. The membrane was lithiated by first soaking the membrane in 300 mL of 80 °C aqueous 0.5 M H_2SO_4 for 2 h followed by 300 mL of 80 °C aqueous 1 M LiOH for 2 h. The membrane was then soaked in 300 mL of 80 °C DI water three times for 30 min each time. Finally, the membrane was dried in a convection oven at 80 °C 24 h. Membranes were stored in a dry box until use.

2.6. NMR

Proton nuclear magnetic resonance (^{1}H NMR, Varian 600 MHz) spectroscopy was performed using DMSO-d_6 (min. 99.8% deuterated, Millipore) as the solvent for POATS and using $CDCl_3$ (99.8% deuterated, Cambridge Isotope Laboratories) as the solvent for Br-PPO. For each measurement, 10 mg of sample was dissolved in 700 μL of the deuterated solvent.

2.7. Thermal analysis

Thermogravimetic analysis (TGA) was performed using a TA instruments TGA Q50 to determine the amount of inorganic material in the POATS samples. A target of 20 mg of sample material was placed in the instrument, and the temperature was ramped to 120 °C at a rate of 20 °C min^{-1} and subsequently held at 120 °C for 45 min to dry the sample. Then, the temperature was increased to 800 °C at a rate of 10 °C min^{-1} under air, to burn away the organic component of the sample. The remaining mass at 800 °C was taken to be the inorganic material present in the POATS. This mass was normalized with the sample mass at the end of the drying step to obtain the mass fraction of inorganic material in the dry POATS.

2.8. Ion exchange capacity

The ion exchange capacity (IEC) was determined using a titration method. Due to the low swelling and possible chemical instability of the membranes under highly acidic conditions, relatively low concentrations of acid and salt were used [35]. First, membranes were dried under vacuum for at least 24 h at 80 °C and weighed. Next, the membranes were soaked in 0.1 M HCl (ACS reagent, Sigma Aldrich) for 6 h at room temperature. Then, they were soaked in DI water twice for 30 min each time, and finally, they were soaked in 0.1 M $CaCl_2$ (ACS reagent, Amresco) solution for 16 h. The membranes were removed, and the $CaCl_2$ solutions were titrated using bromothymol blue (Sigma Aldrich) as an indicator and 0.100 M NaOH (ACS reagent, Macron) as the titrant.

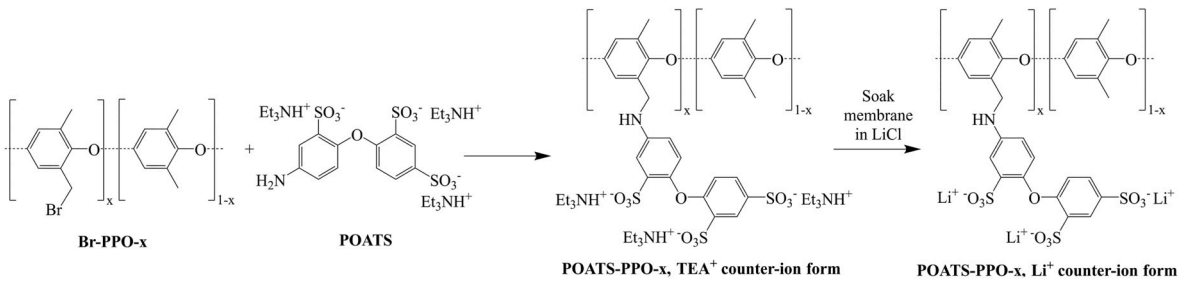

Scheme 3. Preparation of POATS-PPO and conversion to the lithium counter-ion form.

The number of moles of acid in solution was assumed to correspond to the number of equivalents of fixed charge (i.e., sulfonate) groups in the membrane. Then, the IEC was determined by dividing the milli-equivalents of fixed charge groups by the dry mass, in g, of the polymer used in the titration.

2.9. Solvent uptake

To determine solvent uptake, membranes first were dried in an 80 °C vacuum oven for 48 h. The dry mass was recorded, and the samples were immersed in the non-aqueous electrolyte, 1 M LiFSI (Nippon Shokubai) in DMC (99+%, extra dry, Acros Organics), or in DI water for 3 days at room temperature. The samples were wiped, to remove surface liquid, and weighed quickly to determine the solvated sample mass. Solvent uptake was expressed as the percentage increase in mass between the dry membrane and the solvated membrane normalized by the dry membrane mass. To ensure this mass was representative of the equilibrium solvent uptake and to characterize the dimensional stability of the polymers, some membranes were returned to the solvent and left there for 4 months, and no additional mass change was observed.

2.10. Ionic conductivity

Ionic conductivity was measured using electrochemical impedance spectroscopy (EIS, SP 150, BioLogic) [16]. The measurement was performed by placing the membrane between two halves of a glass cell with a cross-sectional membrane area of 4.52 cm^2 that was subsequently filled with electrolyte (1 M LiFSI in DMC or 1 M LiCl in DI water). Custom aluminum electrodes, which spanned the cross-section of the cell, were inserted on both sides of the membrane, and the impedance response was measured from 1 MHz to 1 kHz with a voltage amplitude of 20 mV and 10 points per decade. The resulting data were fit using a model circuit to obtain the high frequency intercept. The resistance associated with this intercept, R_1, was the sum of the membrane, solution, and cell resistances, which were all in series. The test was repeated with no membrane present in the cell to determine the contribution of the solution and cell resistances, $R_{1,Blank}$, which was assumed to be constant for a given electrolyte. The conductivity of the membrane, σ, in mS cm^{-1} was calculated as:

$$\sigma = 1000 * \frac{L}{A\ \ (R_1 - R_{1,Blank})} \tag{1}$$

where A was the cross-sectional area of the cell in cm^2 and L was the membrane thickness in cm.

2.11. Ferrocene permeability

Ferrocene permeability was determined using a two-chamber glass cell with 1 M LiSFI and 0.1 M ferrocene (98%, Acros Organics) in DMC in one half and 1 M LiFSI in DMC in the other. The two chambers were separated by the membrane. Ferrocene concentration in the receiving chamber was measured using ultraviolet–visible (UV–Vis) spectroscopy, taking advantage of the unique ferrocene absorbance peak at 442 nm [20]. The magnitude of this peak has a linear relationship with concentration up to at least 10 mM, which was higher than any concentrations observed in the cell chamber of interest during permeability measurements. The solutions in both chambers were stirred, and over the course of two weeks, the receiving chamber solution was removed, the ferrocene concentration was measured using UV–Vis spectroscopy, and then the solution was returned to the chamber. This process was performed three times over the two-week period to obtain the change in the concentration of ferrocene in the receiving chamber solution over time. Plotting those data versus time resulted in a linear relationship, and ferrocene permeability, P, in $cm^2\ s^{-1}$, was calculated as:

$$V_l \frac{dC_2}{dt} = \frac{A\ \ P}{L}(C_1 - C_2) \tag{2}$$

where V_l was the liquid volume of the receiving cell in mL, A was the cross-sectional area of the membrane in cm^2, L was the thickness of the membrane in cm, C_1 was the ferrocene concentration in the donor chamber, and C_2 was the time-dependent ferrocene concentration in the receiving chamber.

2.12. Electrochemical stability of POATS-PPO membranes

The electrochemical stability of the membranes was tested using cyclic voltammetry (CV). The measurement was made by assembling a 2032-type coin cell using a POATS-PPO-6.6 membrane as a representative POATS-PPO-type material. The membrane was soaked in electrolyte (1 M LiFSI in DMC) for 24 h prior to use as the separator in a coin cell. Lithium foil was used as a combination counter/reference electrode and stainless steel was used as the working electrode. A cell was assembled for comparison where the only difference was that a Celgard 2325 separator was substituted for the POATS-PPO membrane. It is noted that in both cells the membrane was in direct contact with both the lithium foil and the stainless steel. The CV sweeps were done from 2.0 V to 4.5 V vs Li/Li^+ at 50 mV s^{-1} for 3 cycles; and cycles 2 and 3 can be found in Supporting Information, Fig. S1. No features were observed in the CV that suggested oxidation or reduction of POATS-PPO membrane constituents and the current densities at all potentials in the POATS-PPO coin cell were lower than those in the cell with a Celgard membrane, suggesting that POATS-PPO membranes were electrochemically stable within the relevant potential window.

3. Results and discussion

3.1. Membrane composition

The POATS-PPO membranes were prepared using Br-PPO as an intermediate, with the intent to replace fully the bromine groups with POATS. Thus, the final degree of POATS substitution was controlled by the Br-PPO degree of bromination (DB), i.e. the percentage of brominated repeat units. The DB was measured using ^1H NMR spectroscopy, and a representative spectrum can be found in Supporting Information, Fig. S2. Peaks at 2.1 and 6.5 ppm were attributed to the aliphatic and aromatic hydrogens, respectively, on the PPO backbone with no bromine present [22,26]. The chemical shifts attributed to these hydrogens change to 4.3 and 6.7 ppm, respectively, with the addition of bromine to one methyl group of the PPO repeat unit. No peak was observed at 6.1 ppm, which indicated that bromine did not substitute at an aromatic position on the PPO repeat unit [22,26]. The DB was calculated using the ratio of the integrated 4.3 and 2.1 ppm peaks as:

$$DB = \frac{2}{1 + \frac{2}{3} * \frac{Peak\ \ (2.1\ \ ppm)}{Peak\ \ (4.3\ \ ppm)}} * 100\% \tag{3}$$

The aliphatic hydrogen peaks were used to determine the DB due to their greater intensity and separation compared to the aromatic peaks.

The upper and lower limits for the extent of PPO bromination and subsequent functionalization with POATS were limited by the mechanical properties of the resulting membranes. The POATS-PPO membranes made with a DB greater than 9.1% became brittle when the membrane was dry. As such, these membranes generally cracked during film casting. POATS-PPO membranes made with a DB less than 4.6% had a different physical appearance, i.e. slightly opaque instead of clear, and they became brittle when exposed to organic solvents, in contrast to higher DB polymers that became more flexible when exposed to organic solvents. Therefore, materials with DBs ranging from 4.6% to 9.1% were considered in this study. Four polymers were synthesized with DBs of 4.6%, 6.3%, 7.2%, and 9.1%.

The number of sulfonate groups added to the phenoxyaniline during the aromatic sulfonation was initially unknown, thus the structure of POATS was determined using ^{1}H NMR spectroscopy (the spectrum can be found in Supporting Information, Fig. S3). Broad peaks at 5.1 and 8.9 ppm result from protons bound directly to nitrogen in the aromatic amine group of the POATS molecule and in the quaternary amine of the triethylammonium cation respectively [32]. The ethyl groups of the triethylammonium also contributed peaks at 1.1 and 3.0 ppm. The remaining six sharp peaks in the 6.3–8.0 ppm region were attributed to the aromatic hydrogens on the POATS molecule [32]. When the peak integrations were normalized using one of the aromatic hydrogen peaks, all six peaks in this region have an integration of approximately 1. This result indicated that each peak only represented one hydrogen. As such, these NMR results were consistent with the presence of six aromatic hydrogens per POATS molecule, which indicates the presence of three sulfonate groups per POATS molecule. The amount of triethylammonium also suggested the presence of three sulfonate groups per POATS molecule. The peak integrations of the ethyl group hydrogen peaks were 26.3 and 17.8. These values were close to the peak integrations of 27 and 18 expected in a situation where three sulfonate groups, fully converted to the triethylammonium cation form, were present on each POATS molecule.

Thermogravimetric analysis was used to confirm that the inorganic salts used in the purification procedure were removed. The POATS product was heated in air to burn off the organic components. The residual mass, which was taken to be the inorganic matter, which was measured to be less than 1% of the initial dry polymer mass. This result indicated that the calcium sulfate and calcium carbonate were successfully removed during the POATS purification process.

The final POATS-PPO polymers were insoluble in a range of deuterated solvents, so ^{1}H NMR spectroscopy could not be used to determine the amount of POATS added to each polymer. Rather, the ion exchange capacity (IEC) of the polymer was measured to provide quantitative insight into the extent of sulfonation. A comparison of the measured and theoretical IEC values is provided in Table 1. The theoretical IEC was calculated using the DB of the starting Br-PPO and assumed complete substitution of bromine by POATS. The measured IEC values were generally 25%–32% lower than the theoretical IEC values. Neither a longer reaction time nor a larger excess of POATS increased the measured IEC, suggesting that the extent of the POATS functionalization reaction had reached its limit.

The observed difference between theoretical and measured IEC values was not unprecedented, and similar differences have been reported for PPO-based polymers containing a charged side chain [25]. These differences between theoretical and measured IEC values may be a consequence of the titration-based IEC measurement. If some fraction of the sulfonate groups were embedded in the otherwise hydrophobic polymer matrix, those charged groups may be effectively inaccessible (and thus not measured) during the titration-based IEC measurement. This situation, which has been observed in other sulfonated polymers [36], would result in a measured IEC that was lower than the theoretical IEC.

Table 1
Comparison of the theoretical and measured IEC values.

Sample	Theoretical IEC[a] (meq g dry polymer^{-1})	Measured IEC[b] (meq g dry polymer^{-1})
POATS-PPO-4.6	0.99	0.75 ± 0.01
POATS-PPO-6.3	1.29	0.96 ± 0.01
POATS-PPO-7.2	1.43	1.08 ± 0.04
POATS-PPO-9.1	1.72	1.17 ± 0.06

[a] The theoretical IEC was calculated using the degree of bromination, measured using ^{1}H NMR and the assumption of full Br-PPO conversion to POATS-PPO.

[b] Measured IEC was determined from titration data and reported as the average of three samples (with the uncertainty taken as one standard deviation from the mean).

3.2. Membrane dimensional stability and electrolyte uptake

To be viable for organic flow battery applications, the membranes must be dimensionally stable while in contact with non-aqueous (organic) electrolytes (i.e., 1 M LiFSI in DMC in this study) for an extended period of time. This dimensional stability was quantified by measuring solvent uptake. Organic electrolyte uptake was measured as a function of time, and the solvent uptake, for all the membranes considered, generally stabilized after about 12 h. This stabilized value did not significantly change over a subsequent four months of immersion. These results provided evidence that the membranes were chemically and dimensionally stable in the electrolyte, addressing an issue reported for other membranes in organic solvents [37].

Films cast from unfunctionalized PPO were mechanically robust in the dry state, but they weakened and became more brittle when exposed to DMC solvent. In contrast, the POATS-PPO membranes became more flexible upon exposure to DMC. Previous PPO functionalization studies have reported that, while unfunctionalized PPO forms a semi-crystalline polymer, functionalized PPO often becomes amorphous and, in some cases, has a lower glass transition temperature than unfunctionalized PPO [23,38,39]. Crystalline domains in unfunctionalized PPO could restrict the ability of the polymer to swell in DMC, and the additional tension on the polymer chains in this situation could cause unfunctionalized PPO to become more brittle upon exposure to DMC. A reduction in crystallinity upon functionalizing PPO could remove this source of chain tension and may explain the observation that the POATS-PPO materials were more flexible than the unfunctionalized PPO polymer upon exposure to DMC. The POATS-PPO membranes, which were the focus of this study, were mechanically stable in contact with all solvents used, which facilitated further characterization of ionic conductivity and ferrocene permeability.

Water uptake by the POATS-PPO membranes (Fig. 2a) was similar to other PPO-based IEMs reported in literature [21,22,25], and water uptake increased with increasing IEC. The relationship between water uptake and IEC was generally consistent with observations reported for a wide range of charged polymers [40]. The POATS-PPO water uptake, however, was relatively low compared to that of the Nafion®-based membranes used in this study. Nafion® 117, which had been pretreated and converted to the lithium counter-ion form, had more than double the water uptake of any POATS-PPO membrane. The Nafion®/PVDF membrane, also in the lithium counter-ion form, had approximately the same water uptake as POATS-PPO-7.2 even with an IEC less than half that of POATS-PPO-7.2 (0.45 compared to 1.08 meq g dry polymer^{-1}). This phenomenon was observed and reported previously, and was attributed to a greater separation of the hydrophilic and hydrophobic domains in perfluorinated polymers compared to hydrogenated polymers [41].

Solvent uptake significantly changed when the solvent was switched from water to the organic electrolyte (Fig. 2b), the solvent uptake of Nafion® 117 decreased while all other polymers had increased solvent uptake. This difference in behavior may have been caused by the interactions of the solvent with the polymer backbones. Unfunctionalized PPO did not sorb a detectable amount of water, but did swell by 29.5 wt % in organic electrolyte, which indicated that PPO has a significantly higher affinity for DMC compared to water. In contrast, polytetrafluoroethylene (PTFE), which forms the backbone of Nafion®, does not noticeably swell when exposed to either DMC or water. This difference in solvent affinity for the polymer backbone could explain why the organic electrolyte uptake increased compared to the aqueous electrolyte for the POATS-PPO membranes, but decreased for Nafion® 117.

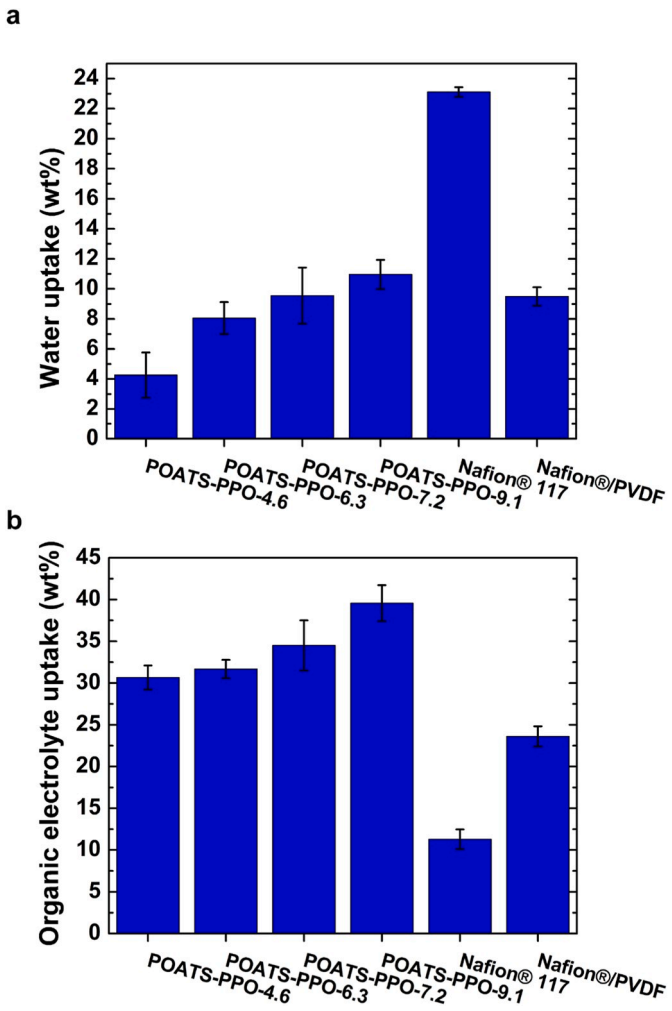

Fig. 2. Mass uptake measured after 3 days using samples initially equilibrated in (a) DI water and (b) 1 M LiFSI in DMC. Longer tests of up to 4 months showed no additional change in swollen sample mass and, thus, uptake. Data are reported as the average of three measurements. The uncertainty was taken as one standard deviation from the mean of the three measurements.

Similarly, a pure PVDF film does not uptake water but swells by about 17 wt% in DMC, which could contribute to the increased swelling of the Nafion®/PVDF membrane in organic electrolyte compared to aqueous electrolyte.

3.3. Ionic conductivity

Ionic conductivities of membranes were measured while immersed in either water or DMC based electrolytes (Fig. 3), with LiCl and LiFSI, respectively, as the added salts. Membrane conductivity was presumed to be largely a result of Li^+ transport because cation transference numbers through negatively charged polymers have been reported to be above 0.8 [42,43]. The POATS-PPO ionic conductivity (in both water and DMC) increased as the IEC of the polymer increased. This result was consistent with generally observed properties of charged polymers [25,26]. Despite the significantly lower water uptake compared to DMC uptake, the POATS-PPO membranes had about an order of magnitude higher conductivity in water than in DMC. This result may be explained by the higher ionic conductivity in aqueous electrolyte than organic electrolytes; the conductivities of the bulk electrolytes used here were measured to be 65 mS cm^{-1} and 7.5 mS cm^{-1} for the aqueous and organic electrolytes respectively.

In contrast, Nafion®/PVDF had 40 times higher conductivity in water than in DMC. For Nafion® 117, which had the most significant difference in uptake between the two solvents, conductivity increased by a factor of 1400 when the solvent was changed from DMC to water. As such, Nafion® 117 had both the highest conductivity in aqueous electrolyte and the lowest conductivity in DMC electrolyte.

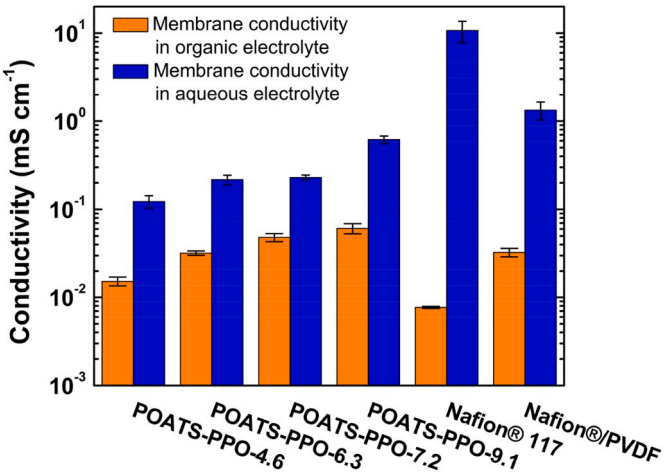

Fig. 3. Ionic conductivity of the POATS-PPO and Nafion®-based control membranes. The values were measured with the membranes immersed in either aqueous electrolyte (1 M LiCl, blue) or organic electrolyte (1 M LiFSI in DMC, orange). Data are reported as the average of three measurements. The uncertainty was taken as one standard deviation from the mean of the three measurements. (For interpretation of the references to colour in this figure legend, the reader is referred to the Web version of this article.)

These differences in conductivity largely follow the trends of solvent uptake, i.e. the membranes with the greatest solvent uptake have the greatest conductivity, with a few exceptions. First, the Nafion®/PVDF membrane had a slightly higher conductivity in aqueous electrolyte than the POATS-PPO membranes for the same water uptake, and a similar conductivity in organic electrolyte with lower organic electrolyte uptake. Second, the POATS-PPO-4.6 and POATS-PPO-6.3 membranes have an approximately twofold different conductivity in the organic electrolyte (0.015 mS cm^{-1} and 0.032 mS cm^{-1}) despite a small difference in solvent uptake (30.7% versus 31.7%).

3.4. Ferrocene permeability

Ferrocene was chosen as the representative redox active molecule in this study because it has been used in RFBs previously [12,20] and has been used as a probe to test membrane crossover [16,44]. Due to the insolubility of ferrocene in water, ferrocene permeability was only characterized using the organic electrolyte (Fig. 4). The ferrocene permeability did not change significantly with increasing IEC of the POATS-PPO membranes. It was reasonable that the IEC of the polymer would not dramatically influence ferrocene permeability due to the molecule being uncharged. The IEC, however, does influence swelling, so ferrocene permeability appeared to also be minimally affected by swelling differences.

The range of the measured ferrocene permeability values, among the POATS-PPO membranes and the Nafion®-based membranes, was much larger than that of the ionic conductivities. While ionic conductivity in DMC varied by less than an order of magnitude across all of the membranes, ferrocene permeability varied by at least three orders of magnitude. The crossover rate in Nafion® 117 was too low to be measured; the ferrocene concentrations remained below the UV–Vis spectroscopy detection limit over the timeframe of the experiment, and thus, an upper limiting value was reported. Ferrocene crossover rates in Nafion® 117 have been reported for other carbonate based electrolytes. In 1 M $LiPF_6$ in propylene carbonate, for example, the crossover rate was

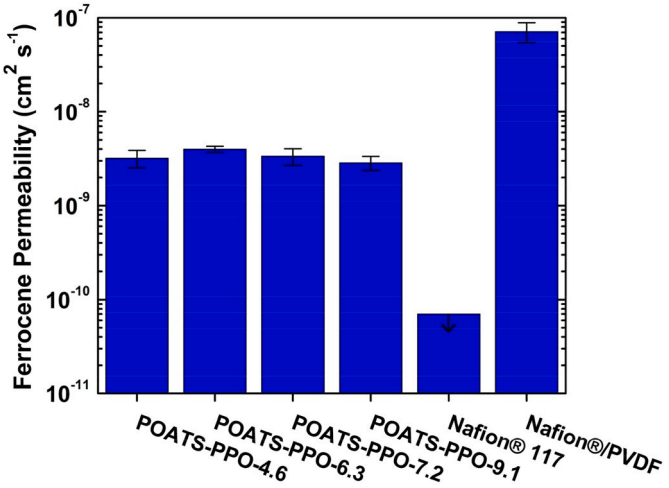

Fig. 4. Ferrocene permeability for the POATS-PPO and control materials. Permeability was measured using 1 M LiFSI in DMC as the electrolyte. Ferrocene permeation through Nafion® 117 was not detectable over the timescale of the measurement, thus the value reported was the upper limit. Data are reported as the average of three measurements. The uncertainty was taken as one standard deviation from the mean of the three measurements.

reported as 8.8×10^{-10} cm^2 s^{-1} [16]. The lower solvent uptake of Nafion® in DMC electrolyte compared to the reported value for this propylene carbonate electrolyte, 11% compared to around 40% [16], may have contributed to a lower observed crossover rate.

The chemical composition and morphology of Nafion® may also have contributed to the relatively low crossover rate. The morphological structure of Nafion® has been described as nano-phase separated hydrophilic and hydrophobic domains [45]. The uncharged and non-polar ferrocene molecule might interact more favorably with the hydrophobic domains. Nafion®, however, is a perfluorinated polymer, and hydrogenated molecules are often excluded from perfluorinated polymers to a greater extent than from hydrogenated polymers [46]. Therefore, ferrocene may experience unfavorable interactions with both the hydrophilic and hydrophobic domains of Nafion®, which could explain the reduced ferrocene permeability relative to that observed in the hydrogenated materials.

The Nafion®/PVDF blended membrane, however, had a much higher crossover rate than the POATS-PPO membranes. This result was consistent with the above speculation; introducing PVDF, a partially hydrogenated polymer, to the membrane yielded an increase in ferrocene permeability, possibly due in part to stronger interactions between ferrocene and the polymer. PVDF also has a low glass transition temperature, −35 °C, which could further drive an increase in ferrocene permeability [47]. In contrast, the POATS-PPO membranes have a hydrogenated, aromatic backbone, which was chemically similar to the aromatic groups of ferrocene, and this chemical similarity may cause the ferrocene permeability to be higher in POATS-PPO compared to Nafion® 117. Confirmation of the speculations surrounding the interactions between the polymer materials and ferrocene was beyond the scope of this study, but understanding the fundamental underpinnings of these differences in crossover will likely be important for designing future RFB membranes with lower crossover rates.

The permeability of the redox active molecule affects the coulombic efficiency, as well as the lifetime of the electrolyte before the concentration of the redox active molecule drops too low, due to crossover, to efficiently charge/discharge the battery [14]. The coulombic efficiency along with the voltage efficiency, which results largely from the membrane conductance, determine the energy efficiency of the battery [3]. To raise both voltage and coulombic efficiency simultaneously, the selectivity, i.e. the ratio of conductivity to active species permeability, needs to increase. However, the selectivity should be considered in combination with conductivity because although a high selectivity and low conductivity membrane has the potential to achieve high voltage and coulombic efficiency, these performance properties can only be realized at low current densities [48].

The relationship between membrane conductivity and permeability for the materials used in this study are shown in Fig. 5, and lines of constant selectivity are provided to aid comparison. Nafion® 117 had the highest selectivity but the lowest conductivity. In contrast, the Nafion®/PVDF blend had the lowest selectivity of the tested membranes in this system. All of the POATS-PPO membranes considered had similar ferrocene permeability, and thus, selectivity increased modestly with increasing IEC to a maximum of 2.1×10^4 S cm^{-3} s.

Presently, few studies report ferrocene permeability of membranes exposed to organic electrolytes. The values, however, can be compared to selectivity values measured in a different non-aqueous system: vanadium(III) acetylacetonate (as the redox active molecule) and 0.1 M tetrabutylammonium tetrafluoroborate in acetonitrile (as the electrolyte). In this system, Tung et al. [13] found that a commercial Neosepta AHA anion exchange membrane, intended for aqueous systems, had a selectivity of 6.7×10^3 S cm^{-3} s, a Celgard 2325 nanoporous separator had a selectivity of 8.2×10^2 S cm^{-3} s, and a custom aramid nanofiber membrane had a selectivity of 1.2×10^3 S cm^{-3} s. When the aramid nanofiber membrane was coated with alternating layers of negatively and positively charged polymers to create a hybrid IEM/nanoporous membrane, the selectivity increased to 1.4×10^5 S cm^{-3} s, which was comparable to the selectivity observed for Nafion® 117 in this report, although with a significantly higher conductivity (0.1 mS cm^{-1} compared to 0.008 mS cm^{-1}). However, while this study and others have shown promise, it is noted that there is still much room for improvement in membrane selectivity and conductivity. For example, in aqueous vanadium RFBs (a commercialized system), selectivity values can be on the order of 10^6 S cm^{-3} s [49].

Non-aqueous RFBs, in general, have not been studied and developed as extensively as aqueous RFBs. As such, few studies exist on membrane materials designed explicitly with the goal of targeting the multidimensional problems of non-aqueous membranes, namely long-term stability in organic electrolyte solutions/solvents, high ionic conductivity for the charge carriers necessary to operate the battery, and

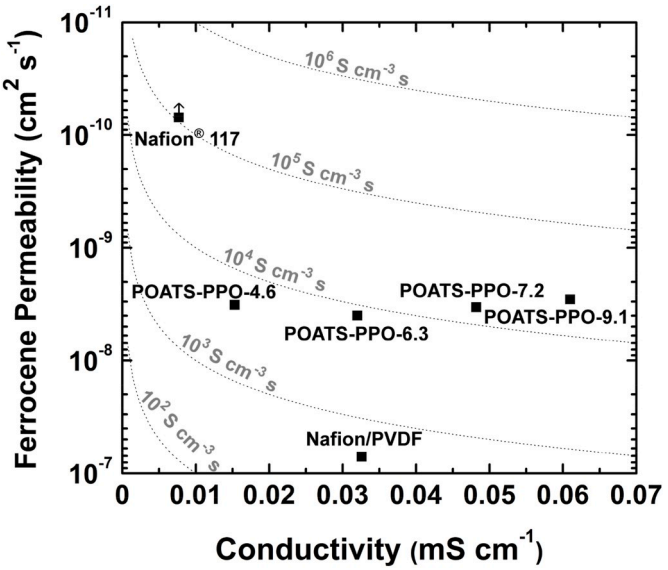

Fig. 5. Ferrocene permeability and membrane ionic conductivity tradeoff plot. Note that the y-axis has been inverted such that permeability decreases (favorable for flow battery applications) in the upward direction. The dashed lines represent different selectivity values, as labeled in the figure. Data points on lines closer to the top right corner have a more favorable ratio of ionic conductivity and ferrocene permeability for RFBs.

limited permeability of the redox active molecules necessary for electrochemical charge/discharge. The material in this report represents one of the few materials explicitly synthesized and characterized towards these often competing material objectives.

4. Conclusions

The vast majority of membrane research has focused on aqueous systems, and thus, ion exchange membranes for non-aqueous systems stand to benefit considerably from continued exploration and optimization of chemistry and processing. Commonly used membranes in aqueous systems do not necessarily maintain their performance and material properties in non-aqueous systems, as suggested by the relative conductivities of Nafion® and POATS-PPO-9 in water and DMC. The comparison of the ionic conductivities of the POATS-PPO membranes and Nafion®-based membranes in aqueous and non-aqueous systems revealed solvent-dependent properties different from that suggested by the intrinsic electrolyte solution conductivities. This result indicated that polymer design strategies for aqueous systems may not scale and transfer to non-aqueous systems in a predictable manner, and improvements in non-aqueous membrane performance may in some cases be achieved by modifying the polymer in a manner that would decrease conductivity measured using an aqueous electrolyte. The POATS-PPO membranes considered in this study achieved an ionic conductivity of up to 0.061 mS cm^{-1}, higher than either of the control membrane materials previously used in non-aqueous redox flow battery applications, while maintaining favorable selectivity properties. Although further work is required to determine which polymer properties have the greatest impact on non-aqueous RFB system performance, the POATS-PPO membranes in this work provide a promising combination of Li^+ conductivity and selectivity, and as more insights are gained into the factors that govern non-aqueous ion exchange membrane performance much potential exists for improvement.

Declaration of competing interest

The authors declare that they have no known competing financial interests or personal relationships that could have appeared to influence the work reported in this paper.

CRediT authorship contribution statement

Patrick M. McCormack: Methodology, Validation, Formal analysis, Investigation, Writing - original draft, Visualization. **Hongxi Luo:** Methodology, Investigation. **Geoffrey M. Geise:** Conceptualization, Writing - review & editing, Supervision, Project administration, Funding acquisition. **Gary M. Koenig:** Conceptualization, Writing - review & editing, Supervision, Project administration, Funding acquisition.

Acknowledgements

This material is based upon work supported, in part, by the National Science Foundation under Grant No. CBET-1752048. PMM acknowledges support from the School of Engineering and Applied Science Dean's Fellowship at the University of Virginia. The authors acknowledge Nippon Shokubai Co., Ltd. for providing the LiFSI used in the organic electrolyte.

Appendix A. Supplementary data

Supplementary data to this article can be found online at https://doi.org/10.1016/j.jpowsour.2020.228107.

Glossary

DB	degree of bromination
DMC	dimethyl carbonate
IEC	ion exchange capacity
IEM	ion exchange membrane
LiFSI	lithium bis(fluorosulfonyl)imide
POATS	phenoxyaniline tri-sulfonate
PPO	poly(phenylene oxide)
PVDF	polyvinylidene difluoride
RFB	redox flow battery

References

[1] P. Alotto, M. Guarnieri, F. Moro, Redox flow batteries for the storage of renewable energy: a review, Renew. Sustain. Energy Rev. 29 (2014) 325–335, https://doi.org/10.1016/j.rser.2013.08.001.
[2] M.L. Perry, A.Z. Weber, Advanced redox-flow batteries: a perspective, J. Electrochem. Soc. 163 (2016), https://doi.org/10.1149/2.0101601jes. A5064–A5067.
[3] A.Z. Weber, M.M. Mench, J.P. Meyers, P.N. Ross, J.T. Gostick, Q. Liu, Redox flow batteries: a review, J. Appl. Electrochem. 41 (2011) 1137–1164, https://doi.org/10.1007/s10800-011-0348-2.
[4] K. Gong, Q. Fang, S. Gu, S.F.Y. Li, Y. Yan, Nonaqueous redox-flow batteries: organic solvents, supporting electrolytes, and redox pairs, Energy Environ. Sci. 8 (2015) 3515–3530, https://doi.org/10.1039/C5EE02341F.
[5] X. Wei, W. Pan, W. Duan, A. Hollas, Z. Yang, B. Li, Z. Nie, J. Liu, D. Reed, W. Wang, V. Sprenkle, Materials and systems for organic redox flow batteries: status and challenges, ACS Energy Lett. 2 (2017) 2187–2204, https://doi.org/10.1021/acsenergylett.7b00650.
[6] W. Wang, Q. Luo, B. Li, X. Wei, L. Li, Z. Yang, Recent progress in redox flow battery research and development, Adv. Funct. Mater. 23 (2013) 970–986, https://doi.org/10.1002/adfm.201200694.
[7] Z. Qi, G.M. Koenig, Z. Qi, G.M. Koenig, Review Article : Flow Battery Systems with Solid Electroactive Materials Review Article : Flow Battery Systems with Solid Electroactive Materials, 2018, 040801, https://doi.org/10.1116/1.4983210.
[8] F.R. Brushett, J.T. Vaughey, A.N. Jansen, An all-organic non-aqueous lithium-ion redox flow battery, Adv. Energy Mater. 2 (2012) 1390–1396, https://doi.org/10.1002/aenm.201200322.
[9] X. Wei, W. Xu, M. Vijayakumar, L. Cosimbescu, T. Liu, TEMPO-based catholyte for high-energy density nonaqueous redox flow batteries, Adv. Mater. 26 (2014) 7649–7653, https://doi.org/10.1002/adma.201403746.
[10] G. Cong, Y. Zhao, Z. Li, Y. Lu, A highly concentrated catholyte enabled by a low-melting-point ferrocene derivative, ACS Energy Lett. 2 (2017) 869–875, https://doi.org/10.1021/acsenergylett.7b00115.
[11] S.E. Doris, A.L. Ward, A. Baskin, P.D. Frischmann, N. Gavvalapalli, E. Chénard, C. S. Sevov, D. Prendergast, J.S. Moore, B.A. Helms, Macromolecular design strategies for preventing active-material crossover in non-aqueous all-organic redox-flow batteries, Angew. Chem. Int. Ed. 56 (2017) 1595–1599, https://doi.org/10.1002/anie.201610582.
[12] B. Hwang, M. Park, K. Kim, Ferrocene and cobaltocene derivatives for non-aqueous redox flow batteries, ChemSusChem 8 (2015) 310–314, https://doi.org/10.1002/cssc.201403021.
[13] S. Tung, S.L. Fisher, N.A. Kotov, L.T. Thompson, Nanoporous aramid nanofibre separators for nonaqueous redox flow batteries, Nat. Commun. (2018), https://doi.org/10.1038/s41467-018-05752-x.
[14] E.C. Montoto, G. Nagarjuna, J.S. Moore, Redox active polymers for non-aqueous redox flow Batteries : validation of the size-exclusion approach, J. Electrochem. Soc. 164 (2017) 1688–1694, https://doi.org/10.1149/2.1511707jes.
[15] M. Doyle, M.E. Lewittes, M.G. Roelofs, S.A. Perusich, R.E. Lowrey, Relationship between ionic conductivity of perfluorinated ionomeric membranes and nonaqueous solvent properties, J. Membr. Sci. 184 (2001) 257–273, https://doi.org/10.1016/S0376-7388(00)00642-6.
[16] L. Su, R.M. Darling, K.G. Gallagher, W. Xie, J.L. Thelen, A.F. Badel, J.L. Barton, K. J. Cheng, N.P. Balsara, J.S. Moore, F.R. Brushett, An investigation of the ionic conductivity and species crossover of lithiated nafion 117 in nonaqueous electrolytes, J. Electrochem. Soc. 163 (2016), https://doi.org/10.1149/2.03211601jes. A5253–A5262.
[17] N.S. Hudak, L.J. Small, H.D. Pratt, T.M. Anderson, Through-plane conductivities of membranes for nonaqueous redox flow batteries, J. Electrochem. Soc. 162 (2015), https://doi.org/10.1149/2.0901510jes. A2188–A2194.
[18] Z. Qi, G.M.K. Jr, A carbon-free lithium-ion solid dispersion redox couple with low viscosity for redox flow batteries, J. Power Sources 323 (2016) 97–106, https://doi.org/10.1016/j.jpowsour.2016.05.033.
[19] S. Wu, Y. Zhao, D. Li, Y. Xia, S. Si, An asymmetric Zn//Ag doped polyaniline microparticle suspension fl ow battery with high discharge capacity, J. Power Sources 275 (2015) 305–311, https://doi.org/10.1016/j.jpowsour.2014.11.012.
[20] C. Jia, F. Pan, Y.G. Zhu, Q. Huang, L. Lu, Q. Wang, High – energy density nonaqueous all redox flow lithium battery enabled with a polymeric membrane, Sci. Adv. 1 (2015) 1–7, https://doi.org/10.1126/sciadv.1500886.
[21] S. Yang, C. Gong, R. Guan, H. Zou, H. Dai, Sulfonated poly(phenylene oxide) membranes as promising materials for new proton exchange membranes, Polym. Adv. Technol. 17 (2006) 360–365, https://doi.org/10.1002/pat.718.
[22] N. Li, T. Yan, Z. Li, T. Thurn-Albrecht, W.H. Binder, Comb-shaped polymers to enhance hydroxide transport in anion exchange membranes, Energy Environ. Sci. 5 (2012) 7888–7892, https://doi.org/10.1039/c2ee22050d.

[23] S.S. Mahajan, Structural modification of poly(2,6-dimethyl-1,4-phenylene oxide), Polym. Plast. Technol. Eng. 30 (1991) 27–36, https://doi.org/10.1080/03602559108019203.
[24] T. Xu, D. Wu, L. Wu, Poly(2,6-dimethyl-1,4-phenylene oxide) (PPO)-A versatile starting polymer for proton conductive membranes (PCMs), Prog. Polym. Sci. 33 (2008) 894–915, https://doi.org/10.1016/j.progpolymsci.2008.07.002.
[25] C.G. Cho, H.Y. Jang, Y.G. You, G.H. Li, S. G, An, Preparation of poly(phenylene oxide-g-styrenesulfonic acid) and their characterization for DMFC membrane, High Perform. Polym. 18 (2006) 579–591, https://doi.org/10.1177/0954008306068118.
[26] Y. Li, J. Sniekers, J.C. Malaquias, C. Van Goethem, K. Binnemans, J. Fransaer, I.F. J. Vankelecom, Crosslinked anion exchange membranes prepared from poly (phenylene oxide) (PPO) for non-aqueous redox flow batteries, J. Power Sources 378 (2018) 338–344, https://doi.org/10.1016/j.jpowsour.2017.12.049.
[27] B. Lafitte, P. Jannasch, Proton-conducting aromatic polymers carrying hypersulfonated side chains for fuel cell applications, Adv. Funct. Mater. 17 (2007) 2823–2834, https://doi.org/10.1002/adfm.200700107.
[28] Z. Du, D.L. Wood, I. Belharouak, Enabling fast charging of high energy density Li-ion cells with high lithium ion transport electrolytes, Electrochem. Commun. 103 (2019) 109–113, https://doi.org/10.1016/j.elecom.2019.04.013.
[29] H.B. Han, S.S. Zhou, D.J. Zhang, S.W. Feng, L.F. Li, K. Liu, W.F. Feng, J. Nie, H. Li, X.J. Huang, M. Armand, Z. Bin Zhou, Lithium bis(fluorosulfonyl)imide (LiFSI) as conducting salt for nonaqueous liquid electrolytes for lithium-ion batteries: physicochemical and electrochemical properties, J. Power Sources 196 (2011) 3623–3632, https://doi.org/10.1016/j.jpowsour.2010.12.040.
[30] M.S. Ding, K. Xu, T.R. Jow, Liquid-solid phase diagrams of binary carbonates for lithium batteries, J. Electrochem. Soc. 147 (2000) 1688–1694.
[31] L. Li, S. Zhou, H. Han, H. Li, J. Nie, M. Armand, Z. Zhou, X. Huang, Transport and electrochemical properties and spectral features of non-aqueous electrolytes containing LiFSI in linear carbonate solvents, J. Electrochem. Soc. 158 (2011) 74–82, https://doi.org/10.1149/1.3514705.
[32] J. Fang, X. Guo, S. Harada, T. Watari, K. Tanaka, H. Kita, K. ichi Okamoto, Novel sulfonated polyimides as polyelectrolytes for fuel cell application: 1. Synthesis, proton conductivity, and water stability of polyimides from 4,4′-diaminodiphenyl ether-2,2′-disulfonic acid, Macromolecules 35 (2002) 9022–9028, https://doi.org/10.1021/ma020005b.
[33] Chemours, Nafion NR211 and NR212, (n.d.). https://nafionstore-us.americommerce.com/Shared/P11_C10610_Nafion_NR-211_NR-212_P11.pdf.
[34] Dupont, DuPont™ Nafion® PFSA membranes, (n.d.) 0–3. http://www.nafionstore.com/Shared/Bulletins/N115-N117-N1110.pdf.
[35] A.R. Khodabakhshi, S.S. Madaeni, T.W. Xu, L. Wu, C. Wu, C. Li, W. Na, S. A. Zolanvari, A. Babayi, J. Ghasemi, S.M. Hosseini, A. Khaledi, Preparation , optimization and characterization of novel ion exchange membranes by blending of chemically modified PVDF and SPPO, Separ. Purif. Technol. 90 (2012) 10–21, https://doi.org/10.1016/j.seppur.2012.02.006.
[36] G.M. Geise, L.P. Falcon, B.D. Freeman, D.R. Paul, Sodium chloride sorption in sulfonated polymers for membrane applications, J. Membr. Sci. (2012) 195–208, https://doi.org/10.1016/j.memsci.2012.08.014, 423–424.
[37] P. Marchetti, M.F.J. Solomon, G. Szekely, A.G. Livingston, Molecular separation with organic solvent Nanofiltration : a critical review, Chem. Rev. 114 (2014) 10735–10806, https://doi.org/10.1021/cr500006j.
[38] T.-P. Jauhiainen, Effect of bromine and phosphorus substituents on the glass transition properties of some substituted poly(oxy-1,4-phenylenes), Angew. Makromol. Chem. 104 (1982) 117–127, https://doi.org/10.1002/apmc.1982.051040111.
[39] Y.S. Bhole, P.B. Karadkar, U.K. Kharul, Nitration and amination of polyphenylene oxide: synthesis, gas sorption and permeation analysis, Eur. Polym. J. 43 (2007) 1450–1459, https://doi.org/10.1016/j.eurpolymj.2007.01.017.
[40] G.M. Geise, D.R. Paul, B.D. Freeman, Fundamental water and salt transport properties of polymeric materials, Prog. Polym. Sci. 39 (2014) 1–42, https://doi.org/10.1016/j.progpolymsci.2013.07.001.
[41] K.D. Kreuer, On the development of proton conducting polymer membranes for hydrogen and methanol fuel cells 185 (2001) 29–39.
[42] H. Zhang, C. Li, M. Piszcz, E. Coya, T. Rojo, L.M. Rodriguez-Martinez, M. Armand, Z. Zhou, Single lithium-ion conducting solid polymer electrolytes: advances and perspectives, Chem. Soc. Rev. 46 (2017) 797–815, https://doi.org/10.1039/c6cs00491a.
[43] Q. Ma, H. Zhang, C. Zhou, L. Zheng, P. Cheng, J. Nie, W. Feng, Y. Hu, H. Li, X. Huang, L. Chen, M. Armand, Single lithium-ion conducting polymer electrolytes based on a super- delocalized polyanion, Angew. Chem. Int. Ed. 55 (2016) 2521–2525, https://doi.org/10.1002/anie.201509299.
[44] L. Yang, J. Zeng, B. Ding, C. Xu, J.Y. Lee, Lithium salt inclusion as a strategy for improving the Li + conductivity of nafion membranes in aprotic systems, Adv. Mater. Interfaces 3 (2016) 1–8, https://doi.org/10.1002/admi.201600660.
[45] K.D. Kreuer, On the development of proton conducting polymer membranes for hydrogen and methanol fuel cells, J. Membr. Sci. 185 (2001) 29–39.
[46] F. Petit, I. Iliopoulos, R. Audebert, S. Szo, Associating polyelectrolytes with perfluoroalkyl side Chains : aggregation in aqueous solution , association with surfactants , and comparison with hydrogenated analogues, Langmuir 7463 (1997) 4229–4233, https://doi.org/10.1021/la970003y.
[47] S.C. George, S. Thomas, Transport phenomena through polymeric systems, Prog. Polym. Sci. 26 (2001) 985–1017.
[48] R.M. Darling, K.G. Gallagher, J.A. Kowalski, S. Ha, F.R. Brushett, Pathways to low-cost electrochemical energy storage: a comparison of aqueous and nonaqueous flow batteries, Energy Environ. Sci. 7 (2014) 3459–3477, https://doi.org/10.1039/C4EE02158D.
[49] Y. Shi, C. Eze, B. Xiong, W. He, H. Zhang, T.M. Lim, A. Ukil, J. Zhao, Recent development of membrane for vanadium redox flow battery applications : a review, Appl. Energy 238 (2019) 202–224, https://doi.org/10.1016/j.apenergy.2018.12.087.